Deltares

Model results of effects of Offshore Wind Farms for MSFD

OWF 2024

Model results of effects of Offshore Wind Farms for MSFD
OWF 2024

Author(s)
Firmijn Zijl
Stendert Laan

Model results of effects of Offshore Wind Farms for MSFD
OWF 2024

Client	Rijkswaterstaat Zee en Delta
Contact	de heer W. van Dijk
Reference	
Keywords	North Sea, offshore wind energy, hydrodynamic modelling

Document control	
Version	1.0
Date	20-12-2022
Project nr.	11208613-002
Document ID	11208613-002-ZKS-0001
Pages	38
Classification	
Status	final

Author(s)

	Firmijn Zijl	
	Stendert Laan	

Summary

Following a similar approach as described in the WOZEP report (Zijl et al., 2021b), Deltares has calculated the hydrodynamic impacts of the expected presence of Offshore Wind Farms (OWFs) in the North Sea in the year 2024. To this end, simulations with the 3D DCSM-FM hydrodynamic model were performed, with and without OWFs. Before this model was applied, it was checked that a required change in software and hardware used did not significantly impact the model quality and output compared to the earlier WOZEP computations and the original model validation.

For the present study, more detailed information on pile density and diameter of the monopiles is available, compared to the earlier WOZEP study. Analysis has shown that this results in a lower combined flow blocking surface in the water column for recent and planned windfarms, compared to the original WOZEP assumptions. Computations with both approaches have shown that the result is a general decrease of computed impacts when using the more detailed approach as used for the present study. This holds in particular for the more recent windfarms with a low pile density and larger diameter of the monopiles.

The report describes expected impacts due to the presence of OWFs with respect to salinity, temperature and the stratification thereof, as well as the M2 tidal amplitude and phase, residual currents and bottom shear stress.

Contents

	Summary	**4**
1	**Introduction**	**7**
1.1	Context	7
1.2	Guide to the reader	7
2	**Model set-up and validation**	**8**
2.1	Model set-up	8
2.1.1	Network and bathymetry	8
2.1.2	Calibration	8
2.1.3	Open boundary forcing	8
2.1.4	Meteorological forcing	8
2.1.5	Freshwater discharges	9
2.2	Comparison to earlier results	9
2.2.1	Performance of modelled water levels	10
2.2.2	Spatial differences	11
3	**Implementation of offshore windfarms**	**13**
3.1	OWF2024 scenario	13
3.2	Parameterization of windfarms	14
3.2.1	General approach	14
3.2.2	Differences in parameterization	14
3.2.3	Impact of change in parameterization	16
4	**Results**	**18**
4.1	Presented parameters	18
4.2	Reference situation (no OWFs)	18
4.2.1	Temperature and salinity	18
4.2.2	Residual currents	20
4.2.3	M2 tide	21
4.2.4	Bed shear stress	22
4.3	Impact of the OWF2024 scenario (annual averages)	22
4.3.1	Salinity	22
4.3.2	Temperature	23
4.3.3	Residual currents	24
4.3.4	M2 tide	25
4.3.5	Bed shear stress	26
4.4	Timeseries of temperature stratification	27
5	**Conclusion**	**29**
5.1	Conclusion	29
5.2	Recommendations	29

References **31**

A Additional figures **32**

A.1 Reference situation (no OWFs, summer averages) 32
A.1.1 Salinity 32
A.1.2 Temperature 33
A.1.3 Residual currents 34
A.1.4 Bed shear stress 34

A.2 Impact of the OWF2024 scenario (summer averages) 35
A.2.1 Salinity 35
A.2.2 Temperature 36
A.2.3 Residual currents 37
A.2.4 Bed shear stress 37

1 Introduction

1.1 Context

In 2020 Deltares has conducted a series of model simulations to determine the environmental impacts of offshore wind farms (OWFs) in the North Sea. This work was part of the WOZEP programme (Wind Op Zee Ecologisch Programma; the Dutch governmental offshore wind ecological programme) and resulted in, among others, a set of difference fields for multiple hydrodynamic parameters. These results are presented in Chapter 3 of Zijl et al. (2021b).

Rijkswaterstaat is responsible for the marine environment in the Dutch North Sea under the Marine Strategy Framework Directive (MSFD – in Dutch: Kaderrichtlijn Mariene Strategie or KRM) of the European Union. For policymaking related to the MSFD, the quantification of hydrodynamic impacts of the OWFs present in 2024 are required. Following the same approach as described in the WOZEP report (Zijl et al., 2021b), Deltares has calculated these impacts, which are presented in the present report. The impacts are quantified with respect to the following hydrodynamic parameters:

- Surface temperature
- Temperature stratification
- Salinity stratification
- Amplitude and phase of the M2 tide
- Residual current magnitude
- Bed shear stress (excluding waves)

1.2 Guide to the reader

In Chapter 2 the model used for the present study is briefly described, both with respect to model set-up as well as changes to the model quality due to a change in software version compared to the original validation and use in the WOZEP study. Subsequently, scenario definition for the present study as well as the parameterization with which OWFs are included in the model are presented in Chapter 3. The results of this study, consisting of the computed impacts of the offshore windfarms on hydrodynamics of the area are presented in Chapter 4. Chapter 5 comprises a brief conclusion and recommendations for future simulations.

2 Model set-up and validation

2.1 Model set-up

For the hydrodynamic modelling described in the present report, the 3D Dutch Continental Shelf Model – Flexible Mesh (3D DCSM-FM) is used. The model version, *dflowfm3d-noordzee_0_5nm-j17_6-v1*, is identical to the one used in the previous study for the WOZEP programme (Zijl et al., 2021b). A detailed description of this model can be found in Zijl et al. (2021a). Key characteristics are presented below.

2.1.1 Network and bathymetry

The 3D DCSM-FM has a horizontal grid resolution of 800m to 900m in the southern North Sea and Dutch coastal waters. The grid resolution decreases towards deeper water and the model boundaries. The vertical discretization consists of 20 equidistantly distributed sigma layers. This implies that each layer has a thickness of 5% of the local water depth, with a layer thickness that varies in space and time depending on the local bed level and water level. The bathymetry in the model mostly originates from the EMODnet 2016 data set. For Dutch coastal waters detailed bathymetric and geometric information is taken from the Baseline database by Rijkswaterstaat. The resulting bathymetry and model extent are presented in Figure 2.1.

2.1.2 Calibration

The bottom roughness in 3D DCSM-FM has been used as a calibration parameter to improve tide propagation. A spatially varying Manning roughness coefficient is determined using data-assimilation techniques by running the model in 2D mode using more than 200 tide gauge stations covering the full model domain.

2.1.3 Open boundary forcing

The open boundary of the model is located off the Northwest European Shelf at 15°W, 43°N and 64°N. Tidal water levels at this boundary are forced using 30 tidal constituents from the global tide model FES2012 (Carrère et al. 2012). Surge water levels at the open boundaries are approximated with a so-called inverse barometer correction, which depends on the local time-varying air pressure. Additional oceanographic forcing at the open boundaries is taken from a global reanalysis[1] by the Copernicus Marine Service (CMEMS). This consists of the sea surface anomaly and temperature and salinity profiles at each boundary forcing location. In addition, these profiles are used as initial conditions to reduce the model's spin-up time.

2.1.4 Meteorological forcing

3D DCSM-FM is coupled with ECMWF's ERA5 global reanalysis (Hersbach et al., 2020) for meteorological forcing from time- and space-varying parameters. For the air-sea momentum flux neutral wind speeds (at 10m) and atmospheric pressure (at MSL) are used. For consistency with ERA5's atmospheric boundary layer a Charnock formulation is used with the Charnock coefficient derived from ERA5's wave model component. The heat flux in the model considers the separate effects of solar (shortwave) and atmospheric (longwave) radiation, as well as heat loss due to back radiation, evaporation and convection. The latter two are computed based on the local air temperature (at 2m), dew point temperature (at 2m) and wind

[1] Global Ocean Physics Reanalysis (https://doi.org/10.48670/moi-00021)

speed. The mass flux through the air-sea interface is included by forcing precipitation and evaporation directly from ERA5.

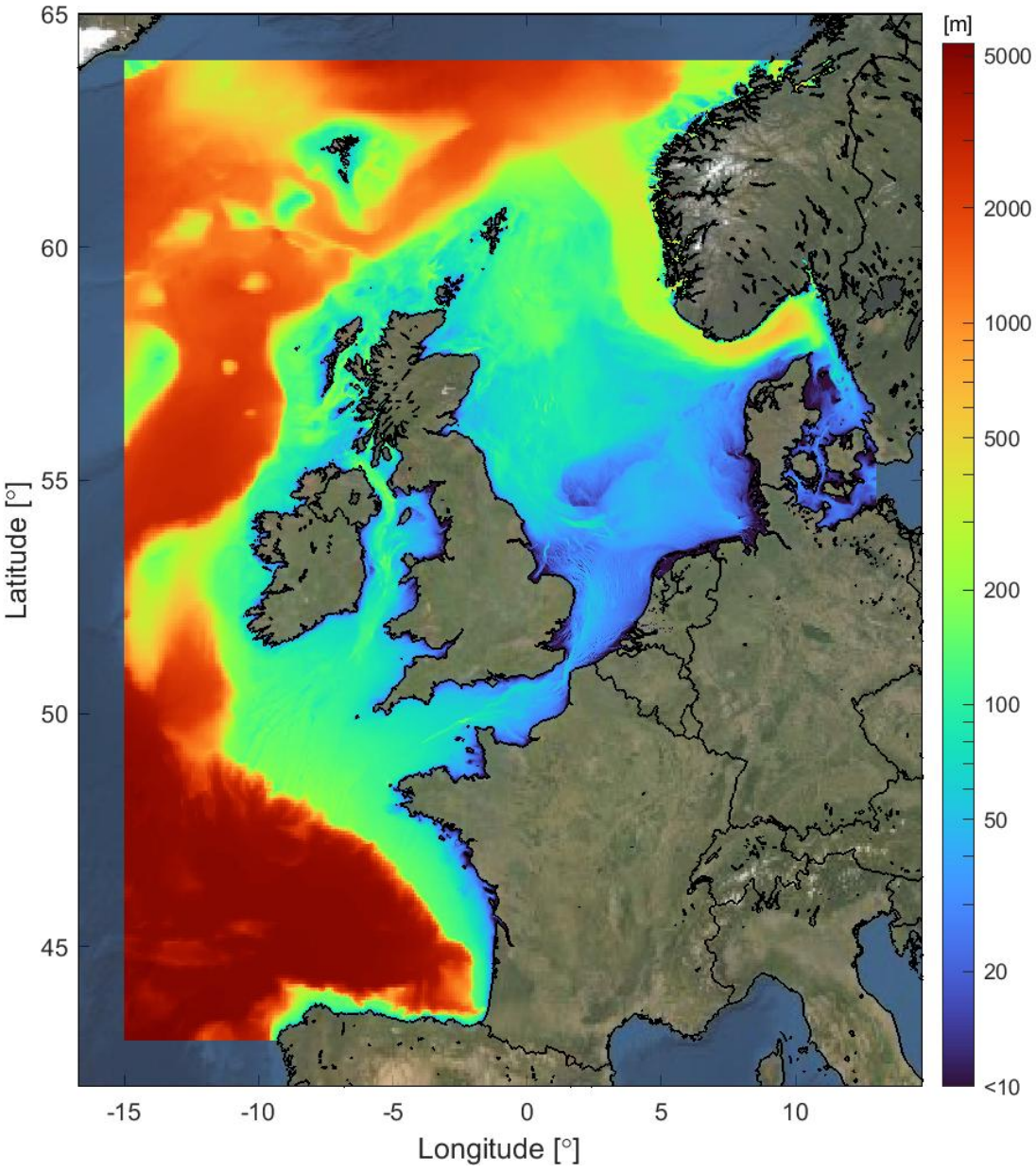

Figure 2.1 Overview of the model bathymetry in 3D DCSM-FM on a logarithmic scale (depth relative to MSL)

2.1.5 Freshwater discharges

Freshwater discharges from rivers are included as a climatological monthly mean discharge rate with associated water temperatures from E-HYPE. The main discharges in the Netherlands and Germany are replaced with observed discharges.

2.2 Comparison to earlier results

An extensive model validation is provided in Zijl et al. (2021a) and will not be repeated here. However, since Deltares has updated the operating system on its computational cluster, it is no longer possible to use the same D-HYDRO software version as was used for WOZEP (and the original model validation). In WOZEP D-Flow FM version 1.2.100.66357 was used, whereas this study uses version 1.2.149.141346. In the present paragraph, a comparison is

made between the model quality of the original and rerun WOZEP reference simulations. The model settings and forcings have not changed.

2.2.1 Performance of modelled water levels

Modelled water levels of both simulations are compared to measurements. To evaluate the quality of the modelled water levels the root-mean-square error (RMSE) is calculated (Table 2.1). Comparing the RMSE of both simulations indicates up to what extent the model quality has changed (Figure 2.2). This change is less than 1 mm in the stations considered and can therefore be considered negligible for the purpose of the present application.

Table 2.1 RMSE of tide, surge and total water level for the original WOZEP simulation and the rerun

Station	RMSE of tide [cm]		RMSE of surge [cm]		RMSE of total [cm]	
	original	rerun	original	rerun	original	rerun
Wandelaar	6.2	6.3	5.0	5.0	8.0	8.0
Zeebrugge Leopolddam	6.0	6.0	4.6	4.7	7.6	7.6
Bol van Heist	6.5	6.6	5.3	5.3	7.5	7.5
Scheur Wielingen	5.9	5.9	4.8	4.9	7.5	7.5
Cadzand	4.8	4.9	4.8	4.8	6.8	6.8
Westkapelle	5.9	6.0	4.5	4.5	7.5	7.5
Roompot Buiten	4.3	4.3	4.6	4.6	6.3	6.3
Brouwershavensegat 8	5.5	5.5	5.2	5.2	7.6	7.6
Haringvliet 10	4.7	4.7	4.9	4.9	6.8	6.8
Hoek van Holland	5.7	5.7	4.9	4.9	7.6	7.6
Scheveningen	5.1	5.1	5.1	5.1	7.2	7.2
IJmuiden Buitenhaven	5.9	5.9	5.3	5.3	7.9	7.9
Den Helder	4.6	4.7	4.6	4.7	6.5	6.6
Texel Noordzee	4.5	4.5	5.2	5.2	7.0	7.1
Terschelling Noordzee	4.4	4.4	4.9	4.9	6.6	6.6
Wierumergronden	4.6	4.7	4.8	4.8	6.6	6.7
Huibergat	5.8	5.8	6.6	6.6	8.8	8.8
Average	5.3	5.4	5.0	5.0	7.3	7.3

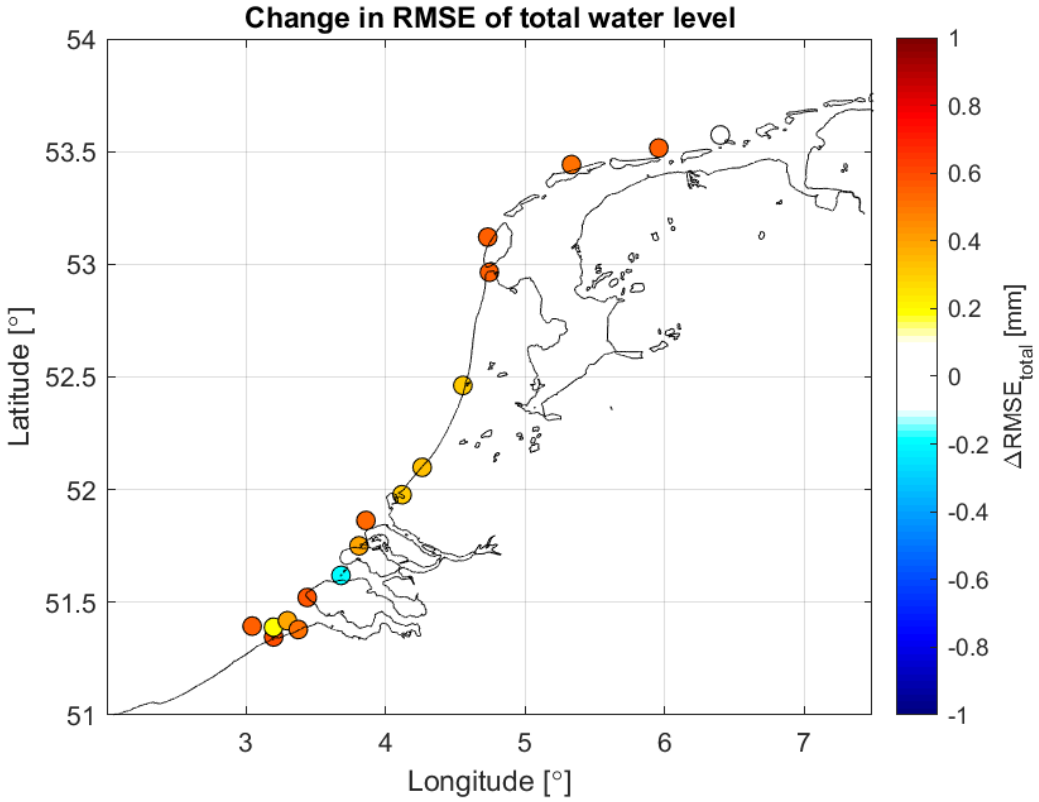

Figure 2.2 Difference in RMSE of total water level between the original WOZEP simulation and the rerun

2.2.2 Spatial differences

In this section spatial differences between both model runs are discussed. These spatial differences are plotted for M2 tidal amplitude (Figure 2.3; left), mean surface velocity magnitude (Figure 2.3; right), mean bottom and surface temperature (Figure 2.4) as well as mean bottom and surface salinity (Figure 2.5). A description of these parameters can be found in section 4.1. The difference fields show virtually no changes in M2 tidal amplitude (Figure 2.3, left) and temperature (Figure 2.4). The velocity pattern (Figure 2.3, right) does show some changes, but only in areas with chaotic patterns of eddies that have apparently shifted in location, such as in deeper oceanic waters and in the Norwegian Trench. Changes in salinity (Figure 2.5) are present in the Kattegat and Baltic Sea. Salinity from the new simulations is slightly higher there (up to 0.4 PSU) at both the bottom and the surface. In this area large gradients can occur between the saline North Sea and the relatively fresh Baltic Sea. This could inflate any small differences between the simulations. With the focus of this study on the North Sea, there is no need to investigate this further.

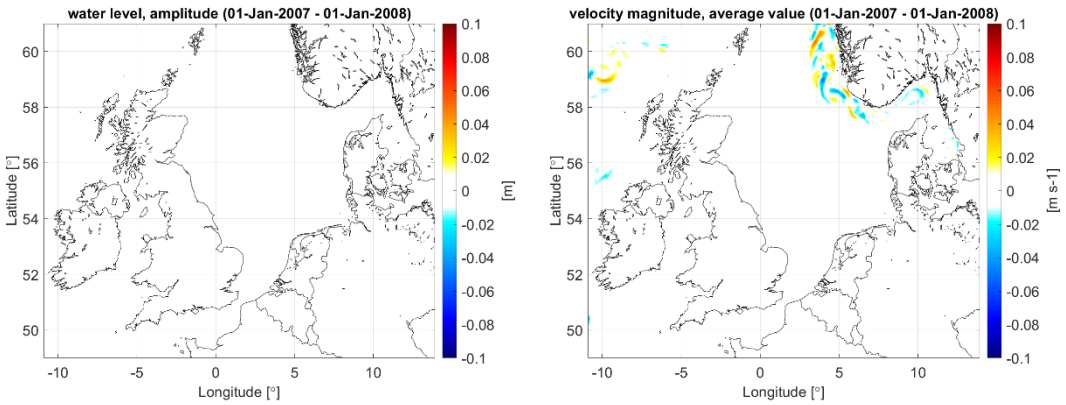

Figure 2.3 Difference between original and rerun of WOZEP reference simulation for 2007; left: M2 tidal amplitude, right: mean surface velocity magnitude

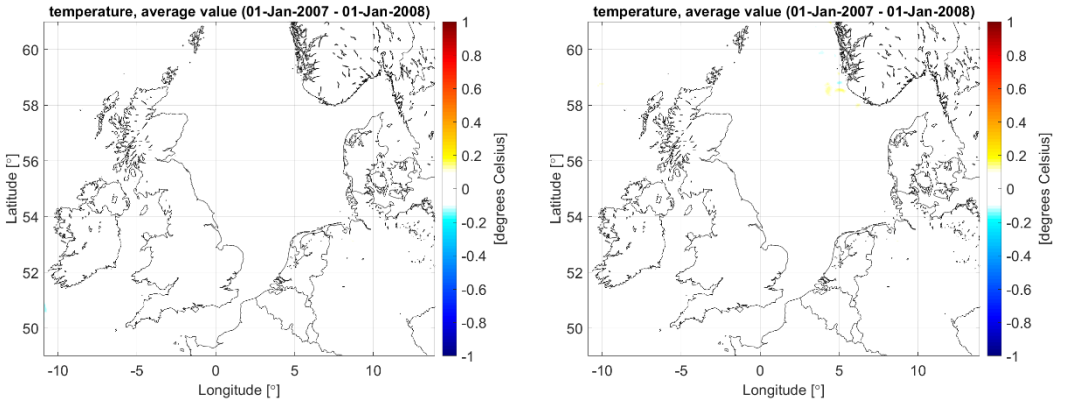

Figure 2.4 Difference between original and rerun of WOZEP reference simulation for 2007; left: mean bottom temperature, right: mean surface temperature

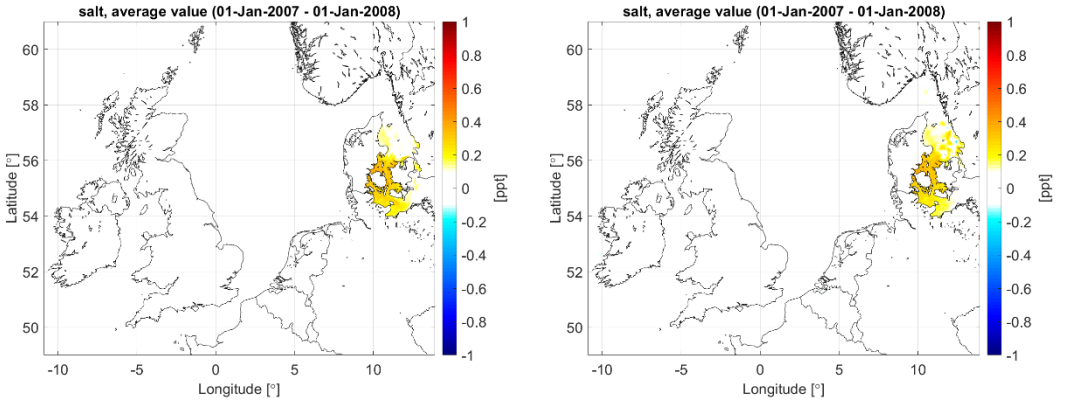

Figure 2.5 Difference between original and rerun of WOZEP reference simulation for 2007; left: mean bottom salinity, right: mean surface salinity

3 Implementation of offshore windfarms

3.1 OWF2024 scenario

A scenario with offshore windfarms in the year 2024 has been provided by Rijkswaterstaat. The location and shape of the windfarms in the North Sea is given in Figure 3.1.

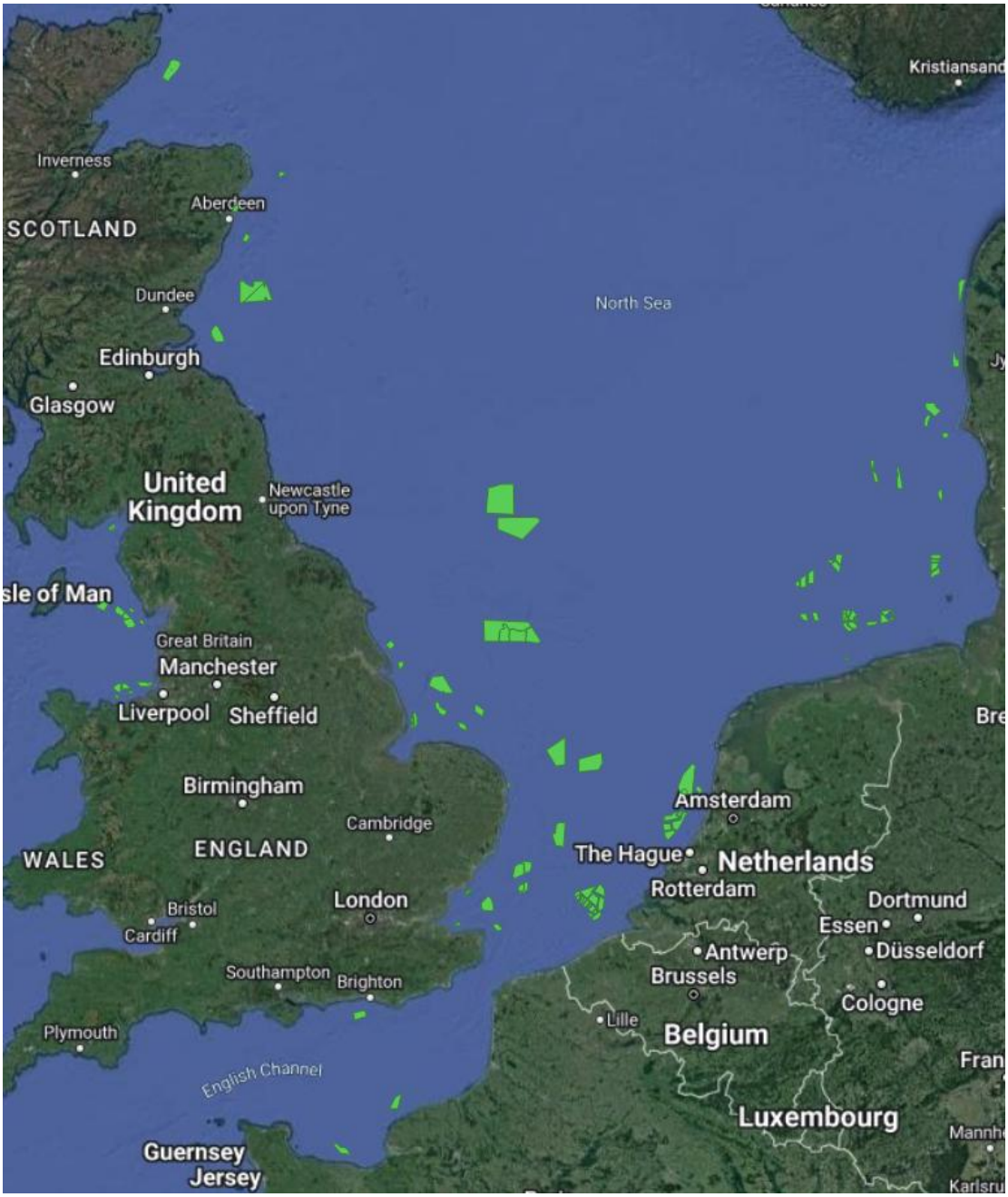

Figure 3.1 Location of windfarms in the 2024 scenario

3.2 Parameterization of windfarms

3.2.1 General approach

With a grid size of 900 m or larger, monopiles of offshore windfarms are too small to explicitly include in the model schematization. Therefore, a sub-grid approach is used. This approach, a quadratic sink term, is included in the horizontal momentum equations. The energy extracted from the main flow in this manner is at the same time reintroduced as a source term in the equation for turbulent kinetic energy (k).

Locations of offshore windfarms are specified in the model by means of a polygon along its boundaries. In each computational cell within this polygon the appropriate sink and source terms are computed considering the pile density (number of piles per unit of area) and the mean pile diameter.

Since the surface applied does not yet include the impact of the windfarms on the meteorological conditions, this has been included in a simplified manner through a 10% reduction of the 10-meter wind speeds (U_{10}) within the boundaries of the wind farms. Other meteorological forcing parameters, such as air temperature and relative humidity, are left unchanged. Wake effects and directional changes of the wind are not considered.

The impact of the windfarms is assessed through the comparison of a scenario computation with a baseline computation. For the modelled period the environmental forcing conditions of the year 2007 have been used, with the year 2006 used for model spin-up. This is the same approach as used in the WOZEP study. The selection of this period was based on several considerations including data availability, the inter-annual variability in temperature stratification in the central North Sea and residual transport through the English Channel.

3.2.2 Differences in parameterization

In the WOZEP study a uniform pile density and diameter of the monopiles was set, based on its construction date. There were three categories:

- Operational in 2020: 3.15 piles/km² with a 5 m diameter
- Under construction in 2020: 0.85 piles/km² with an 8 m diameter
- Future scenario for 2050: 0.67 piles/km² with a 12 m diameter

For this study, more detailed information on the number of turbines per windfarm and the diameter of the monopiles is available. These data are used to include a density (Figure 3.2) and diameter (Figure 3.3) varying per windfarm. Any missing information is completed by taking the average of windfarms with a similar density, diameter or year of construction.

Further analysis has shown that the combined flow blocking width in the water column is on average lower in recent and planned windfarms, compared to the original WOZEP assumptions. This is visualized in Figure 3.4 by multiplying the monopile density with the monopile diameter. The resulting quantity can be seen as the average flow blocking width (due to the presence of monopiles) per square kilometre.

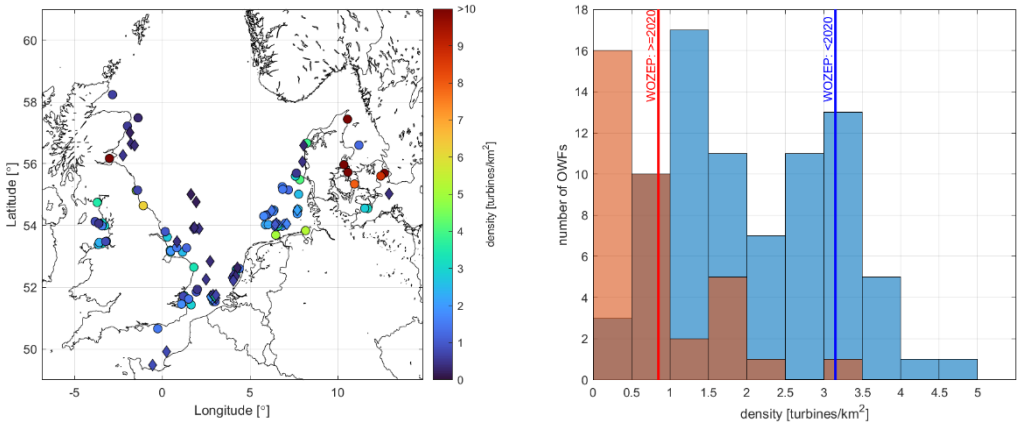

Figure 3.2 Map (left) and histogram (right) of pile density in the windfarms (excluding densities >5 piles/km²). Windfarms constructed before 2020 are presented as filled circles (left) and in blue (right); windfarms constructed in or after 2020 are presented as filled diamonds (left) and in red (right); histograms overlap; the red and blue vertical lines represent the constant densities used in the WOZEP study.

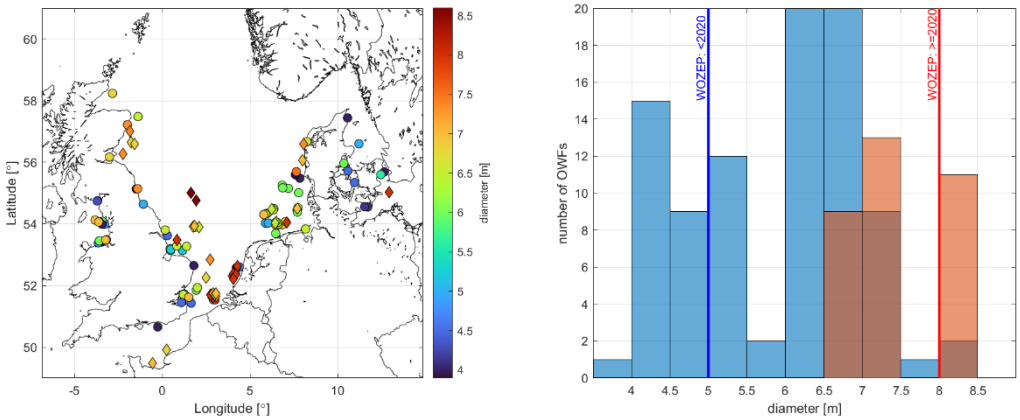

Figure 3.3 Map (left) and histogram (right) of pile diameter in the windfarms. Windfarms constructed before 2020 are presented as filled circles (left) and in blue (right); windfarms constructed in or after 2020 are presented as filled diamonds (left) and in red (right); histograms overlap; the red and blue vertical lines represent the constant densities used in the WOZEP study.

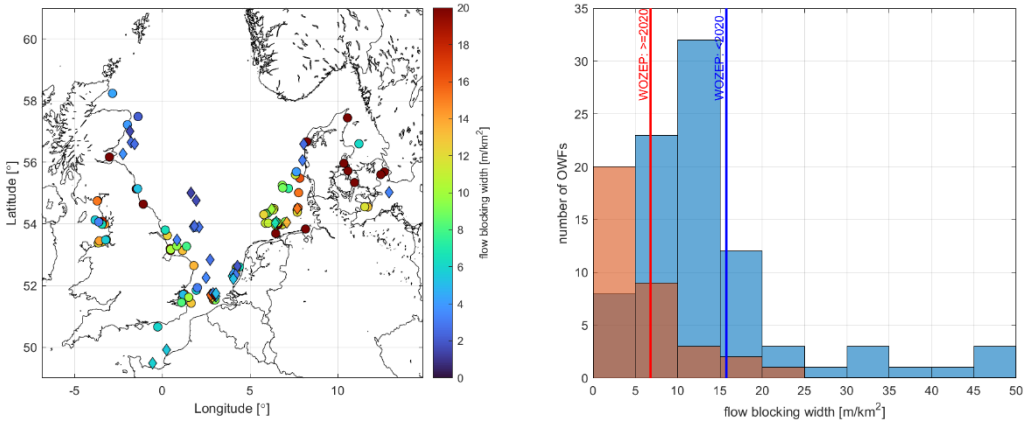

Figure 3.4 Map (left) and histogram (right) of the average flow blocking width per square kilometre in the windfarms. Windfarms constructed before 2020 are presented as filled circles (left) and in blue (right); windfarms constructed in or after 2020 are presented as filled diamonds (left) and in red (right); histograms overlap; the red and blue vertical lines represent the constant densities used in the WOZEP study.

3.2.3 Impact of change in parameterization

The impact of the change to a more detailed parameterization of offshore windfarms is further quantified by computing the impact of the OWF2024 scenario using both parameterizations. A description of the parameters used can be found in section 4.1. Figure 3.5 shows the reduction of the amplitude of the M2 tide in the southern North Sea due to the addition of offshore windfarms. Using the parameterization of the WOZEP study a reduction up to about 3 mm in the German Bight is found. When using the detailed implementation with a varying density and diameter this reduction is about half with a reduction of up to 1.5 mm in the German Bight. This can be explained by the reduced flow blocking surface in the more recent large windfarms, when using the more detailed parameterization.

In Figure 3.6 the change in temperature stratification due to the addition of windfarms using the two different parametrizations is presented. Effects on temperature stratification are mostly local and area specific. Large differences can be seen in the two large British windfarms on the Dogger Bank and the smaller ones in front of the Scottish coast, where temperature stratification reduced by 0.5°C to 2°C using the WOZEP parameterization but is below 0.5°C using the detailed parameterization. In these parks the flow blocking surface is 6.8 m/km² using the WOZEP parameterization, where in the detailed parameterization this is just 2 m/km² to 5 m/km². The lower flow blocking surface results in a reduction of mixing and therefore a smaller effect on the temperature stratification.

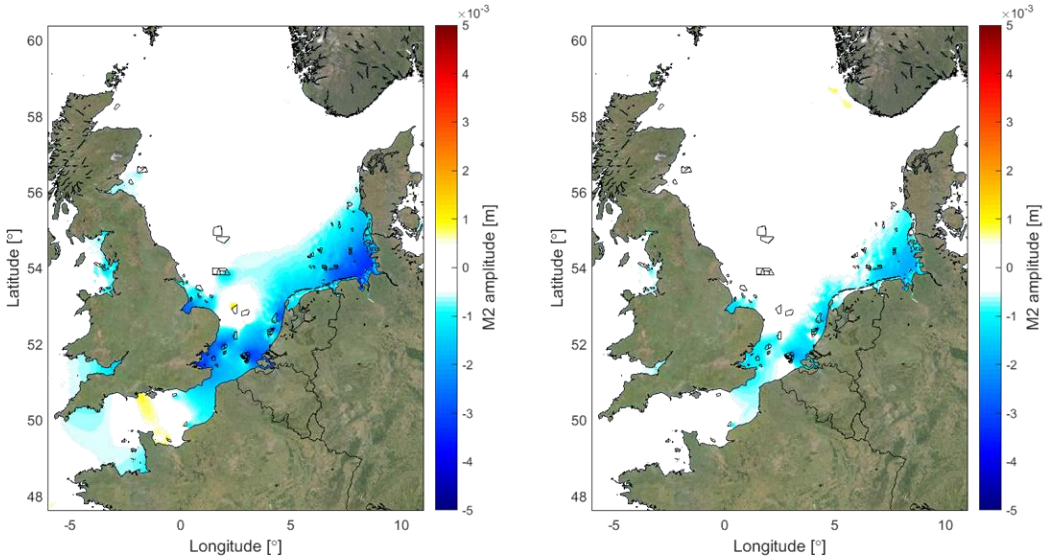

Figure 3.5 Change in M2 tidal amplitude due to the addition of windfarms, using the WOZEP parameterization (left) and the detailed parameterization (right); blue shows a decrease

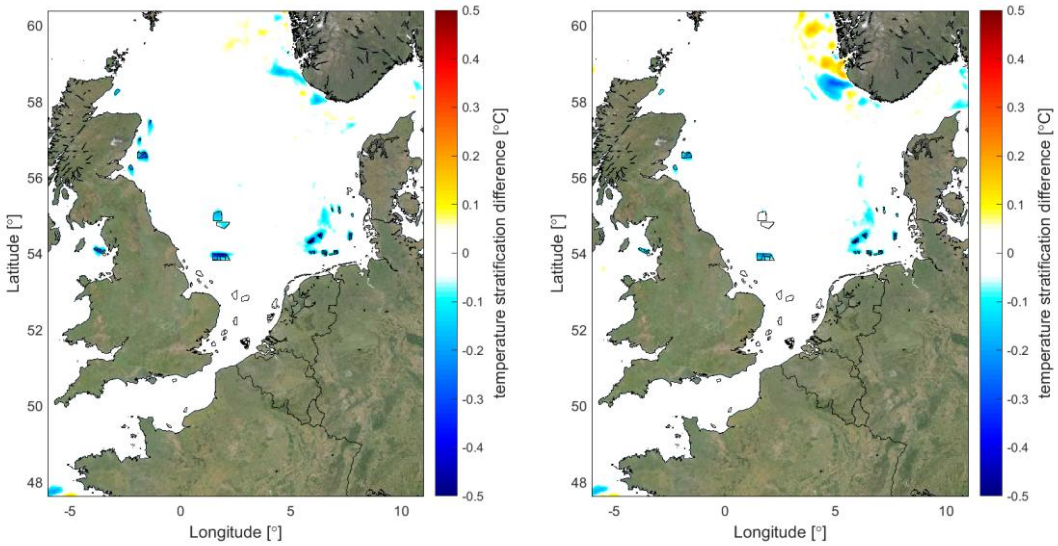

Figure 3.6 Change in temperature stratification due to the addition of windfarms, using the WOZEP parameterization (left) and the detailed parameterization (right); blue shows a decrease

4 Results

4.1 Presented parameters

To assess the effects of offshore windfarms on the hydrodynamics, multiple parameters are determined and compared:

- Surface temperature
- Temperature stratification
- Salinity stratification
- Amplitude and phase of the M2 tide
- Residual current magnitude
- Bed shear stress (excluding waves)

As discussed in section 2.1.1, the model contains 20 equidistant sigma layers throughout the full domain, independent of the local water depth. Where surface or bed values are used, these are taken from the layer highest or lowest in the water column, respectively. This concerns the results for salinity, temperature and residual currents. Salinity and temperature stratification are defined here as the differences between the salinity and temperature values in the top and bottom layers. Water levels (including the M2 tide) and bed shear stress due to currents are two-dimensional quantities, without a vertical component.

For this study, the mean quantities over an entire simulated year (2007) are calculated. In addition, results averaged over the summer months (defined here as July, August and September) are available. To determine the temporal averages over these long periods the 'Fourier' module of D-HYDRO is used. This module calculates the mean values over all simulated timesteps by means of statistical analysis during the model simulation. This allows for an accurate and at the same time storage-efficient model result, since it removes the need to write 3D output at a very high temporal interval for post-processing after the simulation.

Furthermore, the 'Fourier' module allows for a simple tidal analysis. Based on the number of cycles within the analysis time frame, as well as prescribed nodal amplification factor and astronomical argument, an approximation of the spatial field of the M2 tidal amplitude and phase is calculated during the computation.

Effects of the addition of windfarms to the domain are calculated by taking the difference between a simulation without and a simulation with windfarms.

4.2 Reference situation (no OWFs)

Visualizations of the spatial patterns of the annual mean of each presented variable and a brief description thereof are available in Zijl et al. (2021b). For completeness, these fields have been added below based on the reference simulation without windfarms. In the reference scenario, the effect of the offshore wind farms is neglected entirely, including that of the already present wind farms.

4.2.1 Temperature and salinity

In Figure 4.1 the salinity at the bottom and at the surface in the reference situation is presented for the year 2007. Salinity stratification is presented in Figure 4.2. Similarly, this is presented for temperature in Figure 4.3 and Figure 4.4. In these figures the amount of stratification is

determined by subtracting the annual mean value in the top model layer from that in the bottom model layer.

The overall pattern of the stratification is in line with the expected spatial variation (Van Leeuwen et al., 2015). A permanently mixed area is present in the most southern part of the North Sea, between the United Kingdom and the Netherlands. The central North Sea shows a large area with temperature stratification. As expected, temperature stratification (and to some extent salinity stratification) is distinctly reduced in the shallower waters of the Dogger Bank, while mean surface temperatures are higher. Along the coast temperature stratification is weaker due to vigorous tidal mixing, but the effect of the ROFIs attaching to the coast is clearly visible in the salinity stratification.

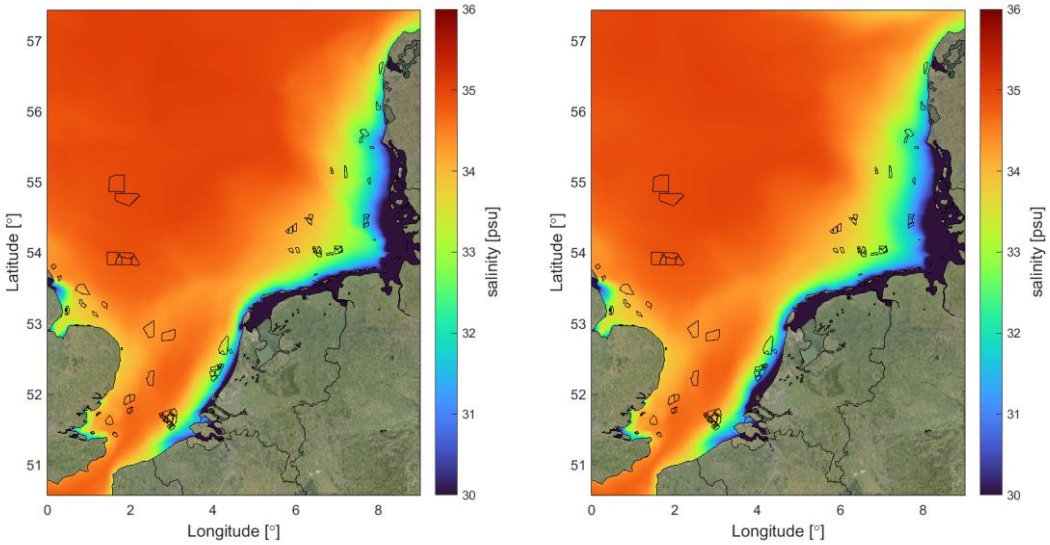

Figure 4.1 Annual mean bottom (left) and surface (right) salinity

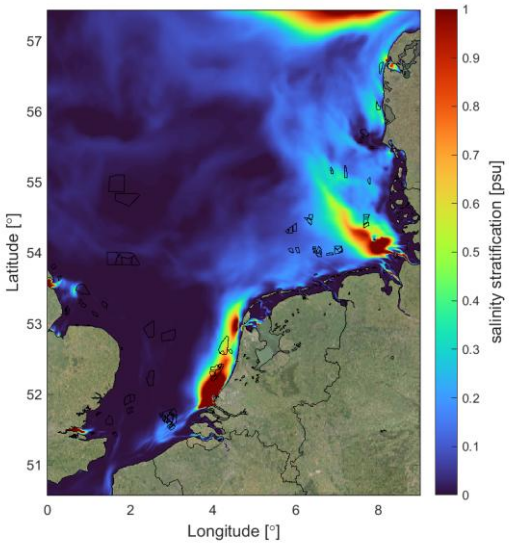

Figure 4.2 Annual mean salinity stratification

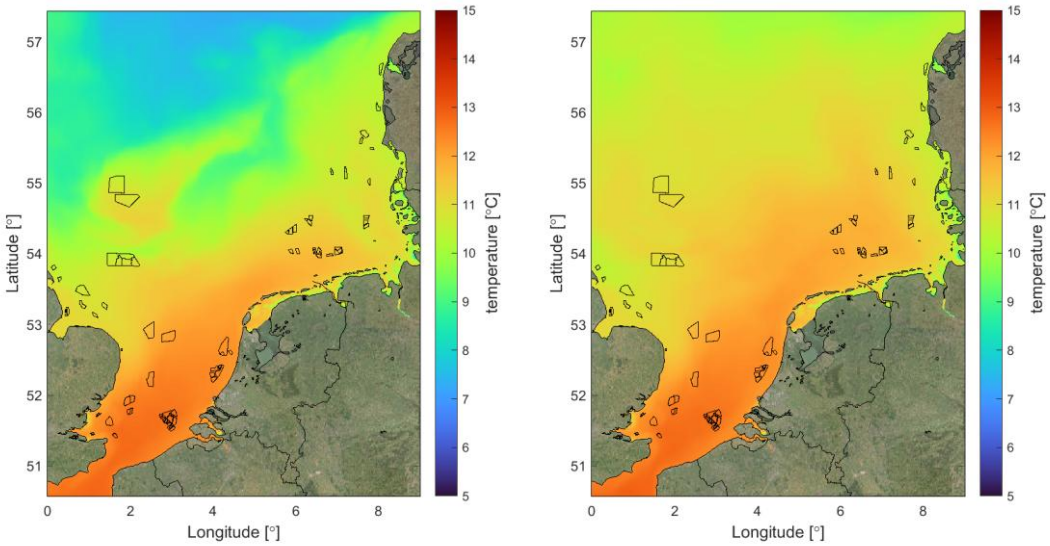

Figure 4.3 Annual mean bottom (left) and surface (right) temperature

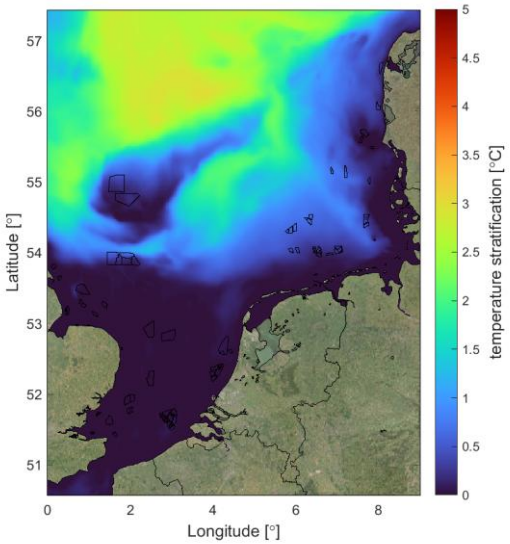

Figure 4.4 Annual mean temperature stratification

4.2.2 Residual currents

In Figure 4.5 the magnitude of the annual mean (residual) currents at the bottom and surface are presented for the year 2007. These show the residual circulation at the surface roughly following a counter-clockwise pattern, with residual current at the bottom much lower than at the surface. As expected, the residual transport through the English Channel is in the direction of the North Sea.

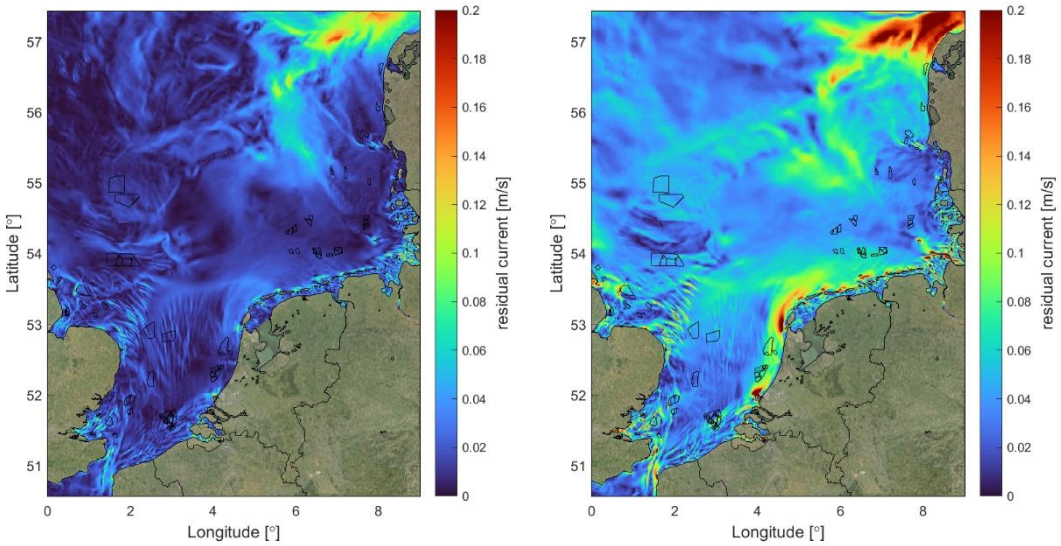

Figure 4.5 Annual mean residual current magnitude at bottom (left) and surface (right)

4.2.3 M2 tide

The semidiurnal lunar M2 tide is the main tidal constituent in most parts of the North Sea. The computed amplitude and phase thereof are presented in Figure 4.6. There figures show the M2 tide behaving as a Kelvin wave, traveling in counter clock-wise direction through the North Sea and with generally higher amplitudes along the coast. Also, clearly visible are the two complete amphidromic systems present in the North Sea, one at a latitude of 52.5° and the other further east near 55-56° latitude. In addition, there is a degenerate amphidromic systems near the southern coast of Norway.

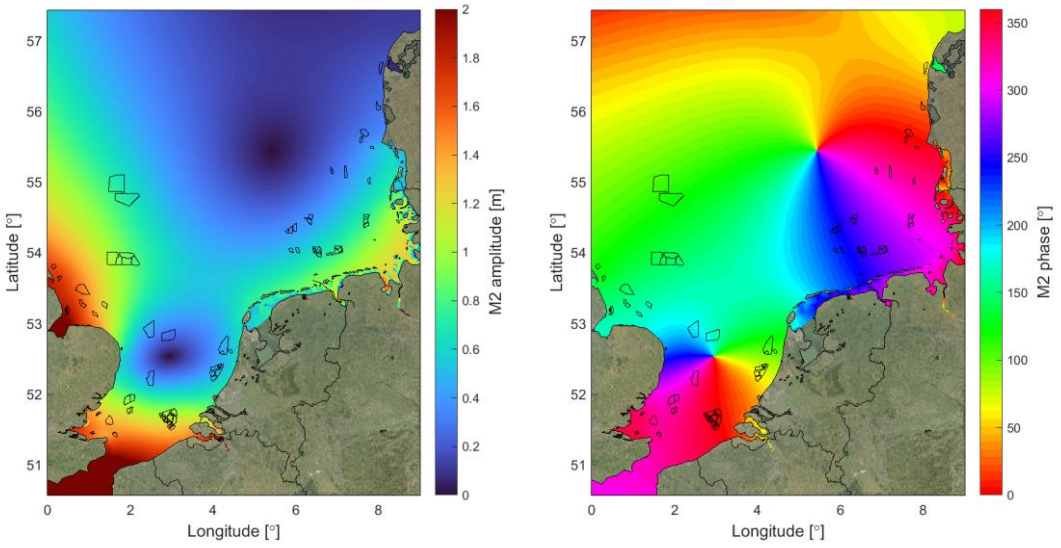

Figure 4.6 Amplitude (left) and phase (right) of the M2 tide

4.2.4 Bed shear stress

The bed shear stress without the effect of waves is presented in Figure 4.7 (left). This shows lower values in the central North Sea, a bit higher values near the shallow coastal waters and in the Wadden Sea and the largest values in the southern North Sea near the English coast. Note that the bed shear stress is strongly influenced by the calibrated Manning roughness fields used in 3D DCSM-FM (Figure 4.7, right). During this calibration, the Manning bottom roughness in 61 areas was adjusted based on measured water levels at 194 shelf-wide tide gauge locations, using a technique available in the open source data assimilation toolbox OpenDA (Zijl & Groenenboom, 2022).

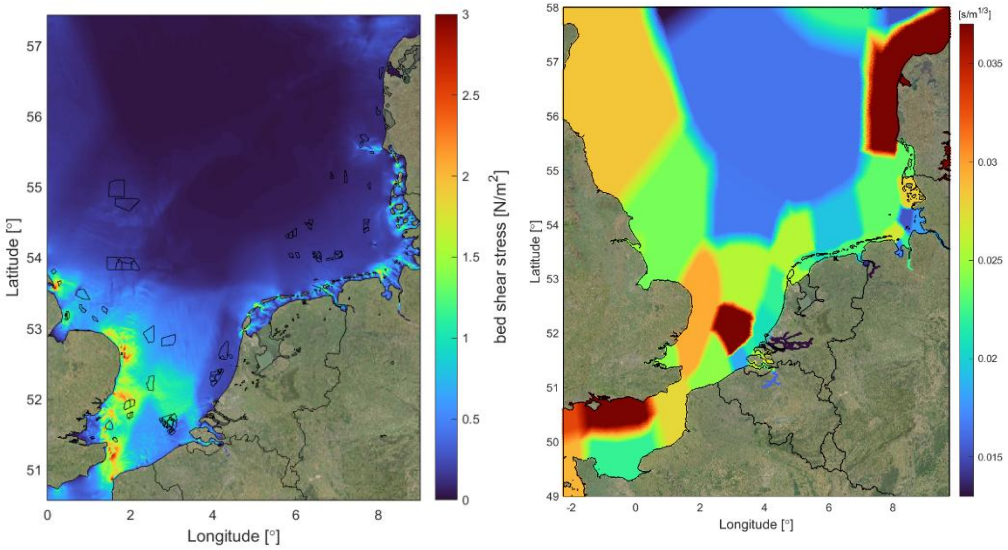

Figure 4.7 Annual mean bed shear stress (left) and calibrated Manning roughness fields in the model (right).

4.3 Impact of the OWF2024 scenario (annual averages)

In this section the impact of the OWF2024 scenario is presented. The impact is quantified by comparing a simulation with windfarms - the OWF2024 scenario as described in Chapter 3 - to a reference simulation without any windfarms. Difference fields of changes are calculated by subtracting the outcome of the reference simulation from that of the OWF2024 scenario simulation. Note that salinity stratification is defined as the bottom value minus the surface layer value, whereas temperature stratification is defined as the surface value minus the bottom layer value. In both cases a resulting positive value contributes to stable density stratification. Relative changes are only shown in the areas where absolute changes are within the visible range of the plotted colormap to avoid indications of large relative changes that are not relevant.

4.3.1 Salinity

Changes in bottom and surface salinity are presented in Figure 4.8, while Figure 4.9 shows the absolute and relative change in salinity stratification. The largest changes are present in the Rhine ROFI off the Holland coast and in the German Bight where the influence of freshwater from river discharges is large. The impact of the OWFs is generally limited to changes of about 0.1 PSU or less. The largest decrease in salinity stratification is about 0.4 PSU and is located in windfarm Hollandse Kust Zuid. This implies a reduction of about 40% of the local annual mean salinity stratification. A slight increase in bottom and surface salinity as well as salinity stratification occurs to the southwest of this windfarm.

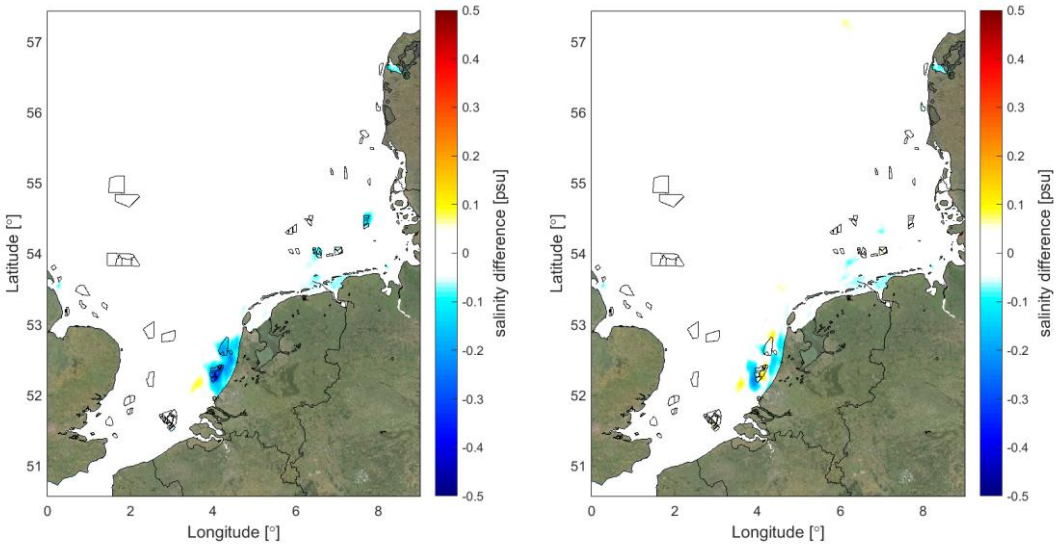

Figure 4.8 Change in annual mean bottom (left) and surface (right) salinity due to the OWF2024 scenario; blue shows a decrease

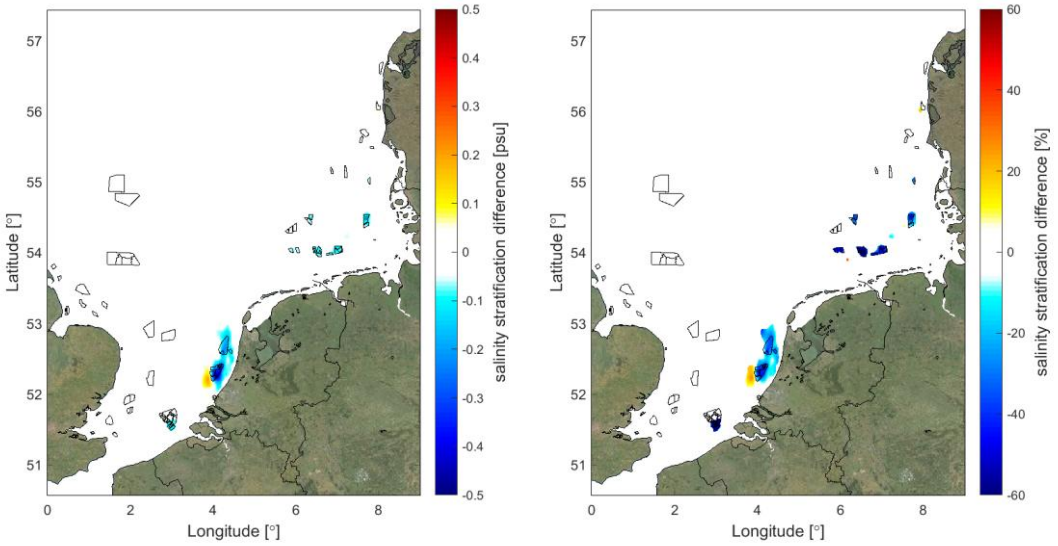

Figure 4.9 Absolute (left) and relative (right) change in annual mean salinity stratification due to the OWF2024 scenario; blue shows a decrease

4.3.2 Temperature

Changes in bottom and surface temperatures due to the OWF2024 scenario are presented in Figure 4.10, while absolute and relative changes in temperature stratification are given in Figure 4.11. These results show that changes are mostly local within and directly surrounding the offshore windfarms. In these areas, bottom temperatures increase with about 0.1°C in windfarms further offshore in British and German waters. In addition, a minimal increase is visible offshore from the German Bight where no windfarms are present. Surface temperatures mostly decrease within the same windfarms with about 0.1°C. An exception is the slight increase in surface temperature in the British windfarms on the Dogger Bank. The largest changes in stratification are found in the most offshore windfarms north of the Wadden Sea

with a reduction of about 0.3°C, which represents about 60% of the local temperature stratification.

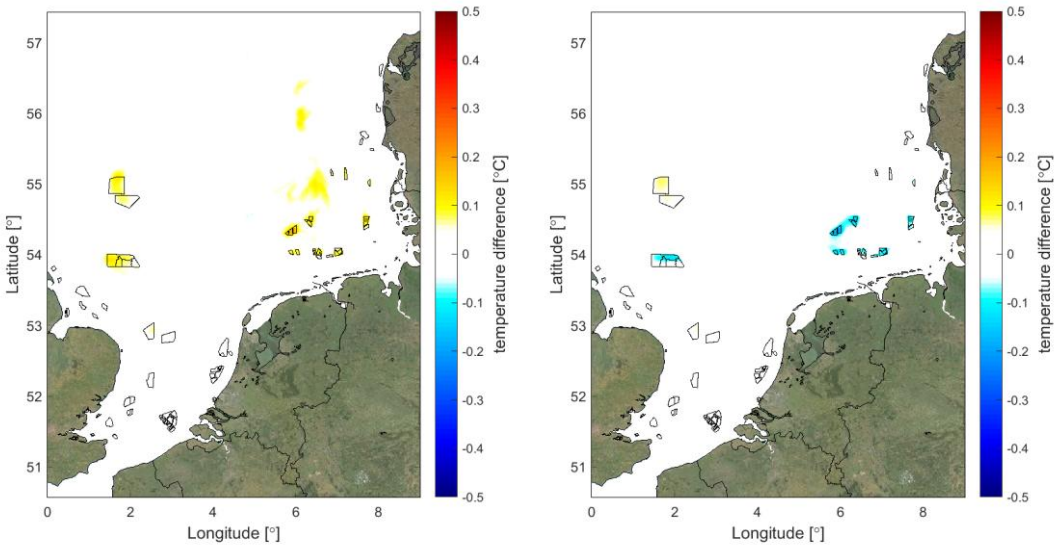

Figure 4.10 Change in annual mean bottom (left) and surface (right) temperature due to the OWF2024 scenario; blue shows a decrease

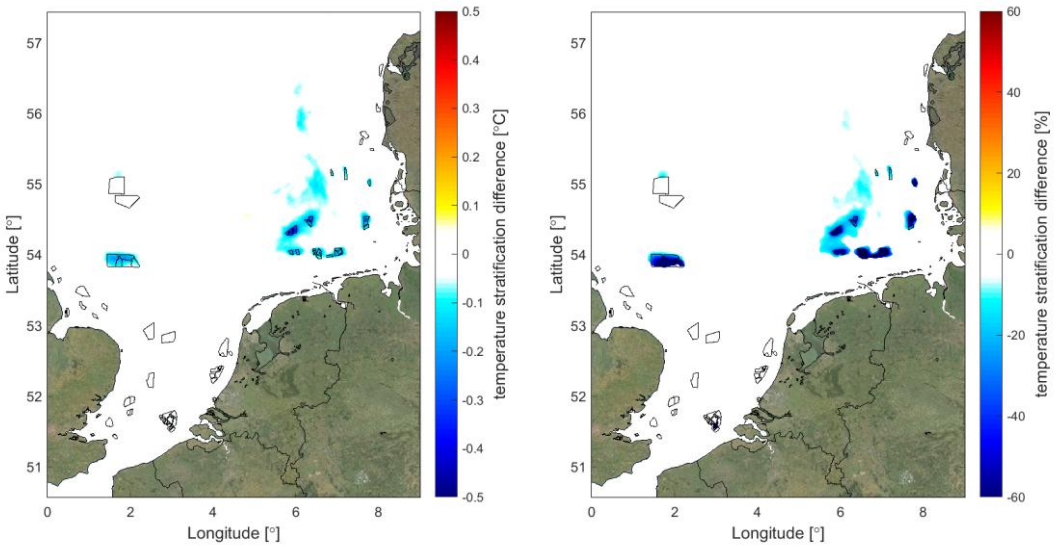

Figure 4.11 Absolute (left) and relative (right) change in annual mean temperature stratification due to the OWF2024 scenario; blue shows a decrease

4.3.3 Residual currents

Changes in residual currents are presented as changes in residual velocity magnitude in the bottom and surface layer (Figure 4.12). The pattern of the coast of Holland is presented in more detail in Figure 4.13. Changes are mainly local with a decrease of about 5 mm/s to 20 mm/s within the windfarms, for the bottom and surface layers respectively. Around and in between windfarms an increase in residual current of roughly the same magnitude can occur. Further

from the windfarms more scattered changes in magnitude show. The general circulation pattern on a North Sea wide scale is hardly affected.

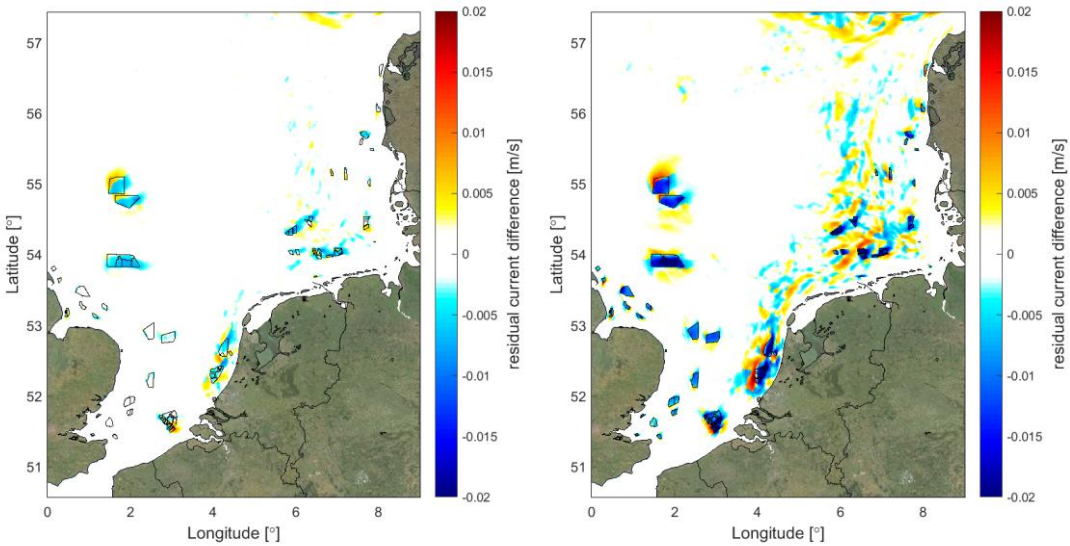

Figure 4.12 Change in annual mean bottom (left) and surface (right) velocity magnitude due to the OWF2024 scenario; blue shows a decrease

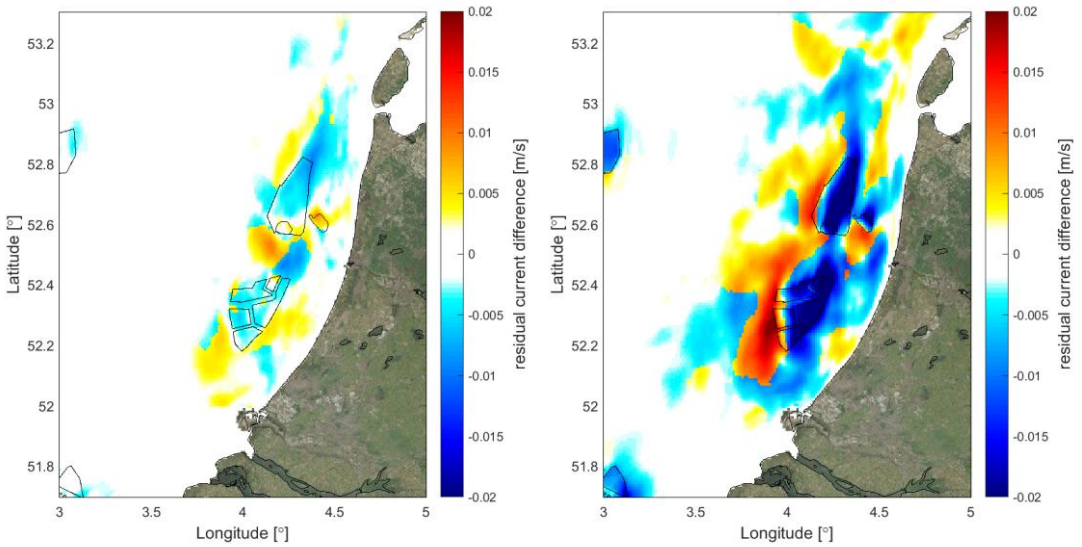

Figure 4.13 Change in annual mean bottom (left) and surface (right) velocity magnitude due to the OWF2024 scenario, zoomed in on the coastal waters of Holland; blue shows a decrease

4.3.4 M2 tide

The spatial pattern of change in the M2 tidal amplitude is presented in absolute and relative sense in Figure 4.14, whereas the change in the M2 tidal phase is given in Figure 4.15. The largest changes in amplitude are found off the Zeeland and Noord-Holland coast and in the German Bight. Maximum changes are about 1.5 mm, corresponding to about 0.2% of the local M2 amplitude. Changes in tidal phase are largest at the two amphidromic points in the southern North Sea, with the sign of these changes reflecting a slight shift in location. Further away from

the amphidromic points, off the Holland coast, the phase increases with about 0.2°. Both a decrease in amplitude and an increase in phase are consistent with the increased dissipations through the drag introduced by the piles in the windfarms.

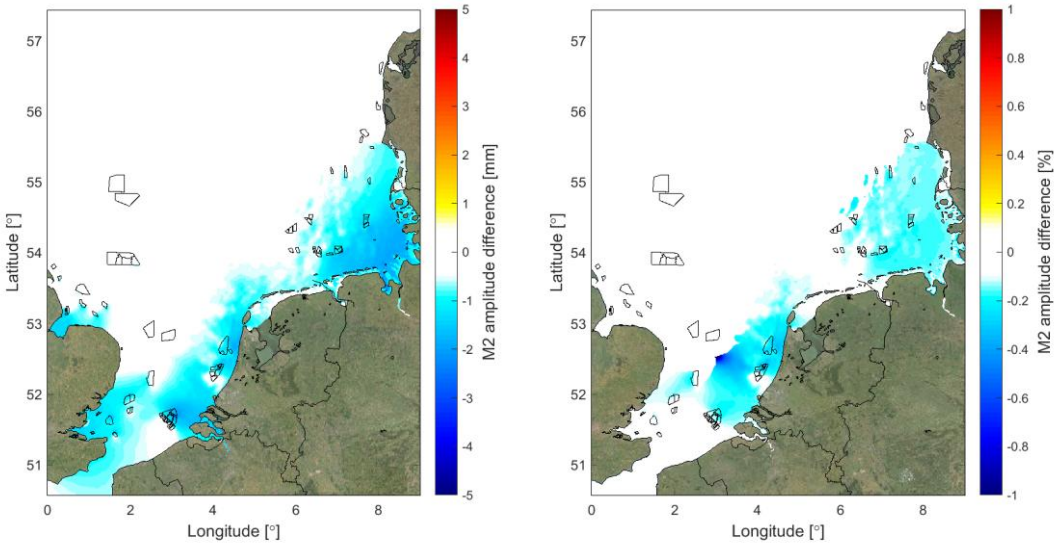

Figure 4.14 Absolute (left) and relative (right) change in amplitude of the M2 tide due to the OWF2024 scenario; blue shows a decrease; note that the absolute change is presented in mm

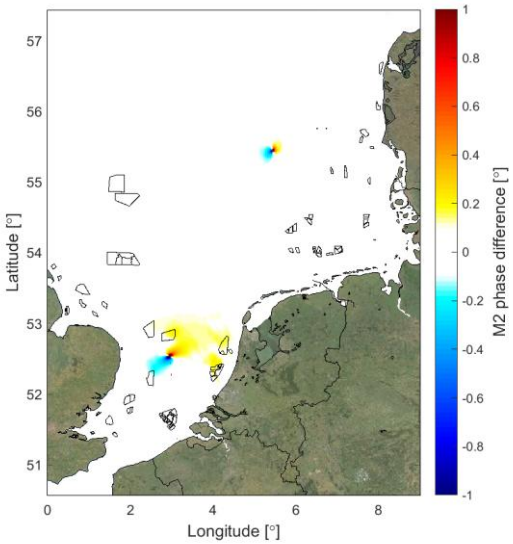

Figure 4.15 Change in the phase of the M2 tide due to the OWF2024 scenario; blue shows a decrease.

4.3.5 Bed shear stress

The absolute and relative change in bed shear stress is given in Figure 4.16. Note that the bed shear stress only contains the effect of currents and excludes the effect of waves. Changes in the computed bed shear stress are local with slight increases of up to 0.04 N/m² within windfarms and slight decreases of less than 0.01 N/m² in the direct vicinity. Changes are largest in the OWFs in the southern North Sea between the Netherlands and the United Kingdom.

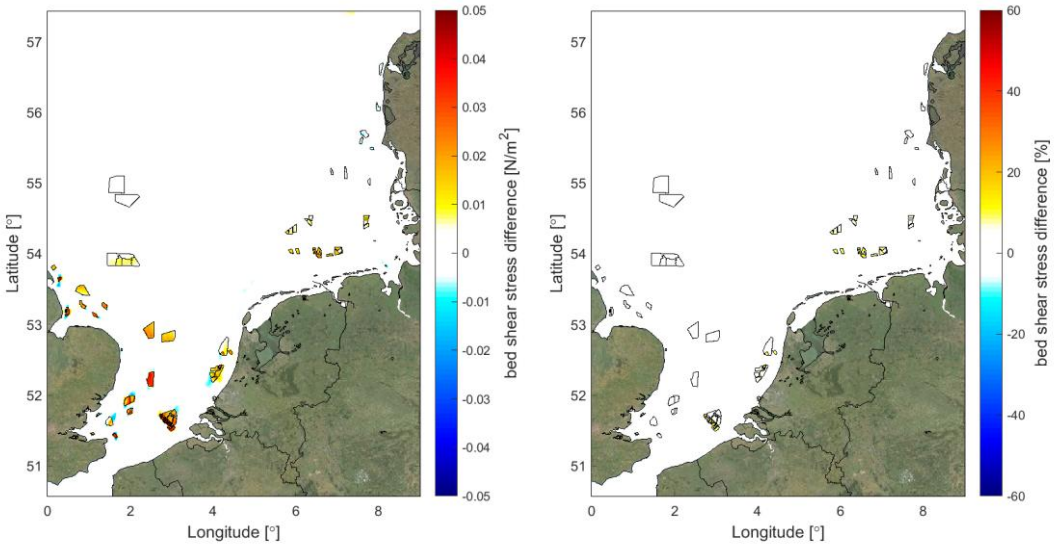

Figure 4.16 Absolute (left) and relative (right) change in annual mean bed shear stress due to the OWF2024 scenario; blue shows a decrease

4.4 Timeseries of temperature stratification

The timeseries in Figure 4.17 show the temporal variation in temperature stratification in 2007 for model output locations in OWFs off the Dutch coast. These are WALCRN30 in the OWF Borssele, NOORDWK30 in the OWF Hollandse Kust Zuid, HKNA in the OWF Hollandse Kust Noord, GeminiWindPark, ROTTMPT100 in the OWF BARD Offshore 1 and FINO1 in the cluster of OWFs of Borkum. In the legend the duration of the temperature stratification is shown, defined at the number of days for which the vertical temperature difference is above 0.5°C (plotted as a dashed line).

At these locations within windfarms, stratification is often intermittent, with a duration of up to several weeks. In general, the presence of windfarms decreases the temperature stratification, also resulting in a reduced period in which significant temperature stratification is present. When the vertical temperature difference without windfarms is around the threshold that we defined (0.5°C), the total duration of the stratification can reduce significantly. Likely this effect is smaller for OWFs in more seasonally stratified regions of the North Sea.

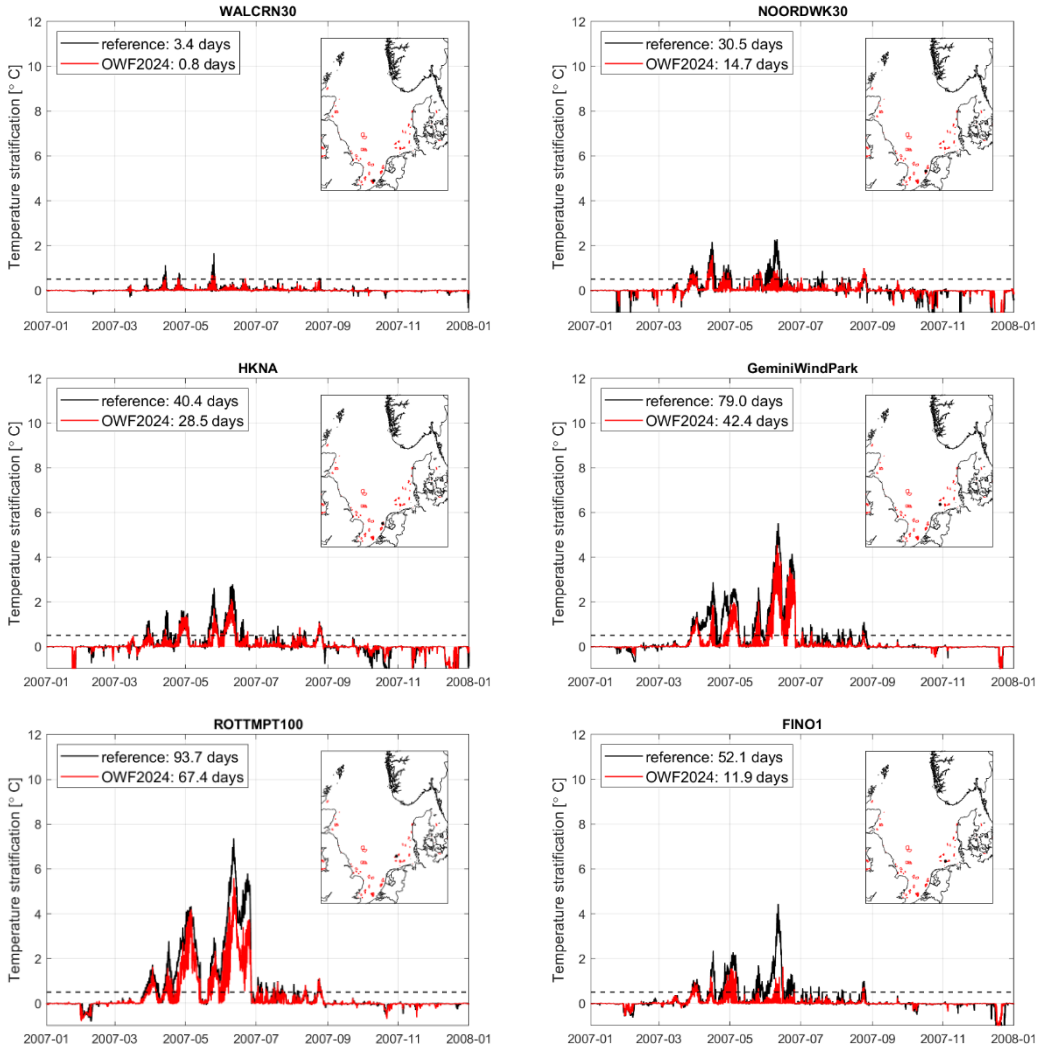

Figure 4.17 Timeseries of temperature stratification in the reference situation (black) and OWF2024 scenario (red) at multiple locations in OWFs off the Dutch coast; locations are marked by a black dot in the included map, exceedance time of the 0.5°C threshold is included in the legend

5 Conclusion

5.1 Conclusion

Following a similar approach as described in the WOZEP report (Zijl et al., 2021b), Deltares has calculated the hydrodynamic impacts of the expected presence of Offshore Wind Farms (OWFs) in the North Sea in the year 2024. To this end, simulations with the 3D DCSM-FM hydrodynamic model were performed, with and without OWFs. Before this model was applied, it was checked that a required change in software and hardware used did not significantly impact the model quality and output compared to the earlier WOZEP computations and the original model validation.

For the present study, more detailed information on pile density and diameter of the monopiles is available, compared to the earlier WOZEP study. Analysis has shown that this results in a lower combined flow blocking surface in the water column for recent and planned windfarms, compared to the original WOZEP assumptions. Computations with both approaches have shown that the result is a general decrease of computed impacts when using the more detailed approach as used for the present study. This holds in particular for the more recent windfarms with a low pile density and larger diameter of the monopiles.

The main conclusions on the hydrodynamic effects of the modelled offshore windfarm scenario are presented below.

- The OWF2024 scenario leads to bottom salinity decreases of about 0.1 PSU to at most 0.4 PSU in and around the windfarms. Surface salinity decreases with about 0.1 PSU to 0.2 PSU, while salinity stratification decreases with a similar magnitude.
- Changes in temperature under the OWF2024 scenario are concentrated in and near the windfarms. Bottom temperatures increase with 0.1°C, while surface temperatures can decrease with about 0.1°C. Temperature stratification decreases with at most 0.3°C.
- Residual currents are impacted with a decrease within the wind farm areas of about 5 mm/s and 20 mm/s, for the bottom and surface layers respectively. Directly surrounding the windfarms an increase of a similar magnitude can be observed. General larger scale circulation patterns in the southern North Sea are not affected.
- The M2 tidal amplitude shows a decrease of up to 1.5 mm off the Zeeland and Noord-Holland coast and in the German Bight. The M2 tidal phase changes around the amphidromic point in the southern North Sea, reflecting a slight shift in its location. Off the Holland coast, but further away from the amphidromic point, an increase of 0.2° is visible.
- Bed shear stresses are increasing slightly with up to 0.04 N/m² within windfarms and slightly decreasing with less than 0.01 N/m² in the direct vicinity of the windfarms.

5.2 Recommendations

The change in parameterization of the offshore windfarms used in this study, compared to the WOZEP approach, has a large influence on the hydrodynamic impacts found. While the current approach seems to better reflect the actual pile diameter and density, it is advised to further study the cause of this effect. Large 3D ecosystem-scale models such as 3D DCSM-FM incorporate a simplified representation of turbulence and turbulent mixing due to the presence of Offshore Wind Farms, in order to keep calculation times within acceptable limits. In a currently running project funded by the National Science Agenda (NWA), more detailed research is carried out on the relationships between pile diameter, decay of vortices behind the

piles and the conversion of energy extracted from the flow into turbulent kinetic energy. These studies are performed with computational fluid dynamics, which resolves the full turbulence spectrum. Such more detailed studies can be instrumental in understanding the underlying physical processes and improving the parameterization of wind farms in large ecosystem-scale models. In addition to the more detailed process modelling, this project is also yielding valuable field data on temperature and salinity profile impacts of offshore wind farms.

Furthermore, future simulations of for example the WOZEP program may be improved by choosing values of the monopile density and diameter closer to the actual characteristics of the windfarms. In any case, a proper comparison with measurement data is still required to validate the computed impact of windfarms and their implementation within the hydrodynamic model.

References

Carrère L., Lyard F., Cancet M., Guillot A., Roblou L., (2012). FES2012: A new global tidal model taking taking advantage of nearly 20 years of altimetry, Proceedings of meeting "20 Years of Altimetry", Venice 2012.

Hersbach, H., Bell, B., Berrisford, P., et al. (2020). The ERA5 global reanalysis. Q J R Meteorol Soc. 146: 1999–2049. https://doi.org/10.1002/qj.3803

Zijl, F., Groenenboom, J. (2019). Development of a sixth-generation model for the NW European Shelf (DCSM-FM 0.5nm). Deltares, report 11203715-004-ZKS-0003, Delft.

Zijl, F., Laan, S.C., Groenenboom, J. (2021a). Development of a 3D model for the NW European Shelf (3D DCSM-FM). Report 11205259-015-ZKS-0003. Deltares, Delft.

Zijl, F., Laan, S.C., Emmanouil A., Kessel, T. van, Zelst, V.T.M. van, Vilmin, L.M. and Duren, L.A. van. (2021b). Potential ecosystem effects of large upscaling of offshore wind in the North Sea: Bottom-up approach. Report 11203731-004-ZKS-0015. Deltares, Delft.

Van Leeuwen, S., Tett, P., Mills, D., and van der Molen, J. (2015). Stratified and nonstratified areas in the North Sea: Long-term variability and biological and policy implications. *J. Geophys. Res.* **120**, 4670-4686.

A Additional figures

The figures presented in Sections 4.2 and 4.3 show annual averages. In additions to these, the same figures are produced with average values over the summer months. These are presented below. This summer-average is determined over the months July, August and September, when temperature stratification in the central North Sea is expected to be largest.

A.1 Reference situation (no OWFs, summer averages)

A.1.1 Salinity

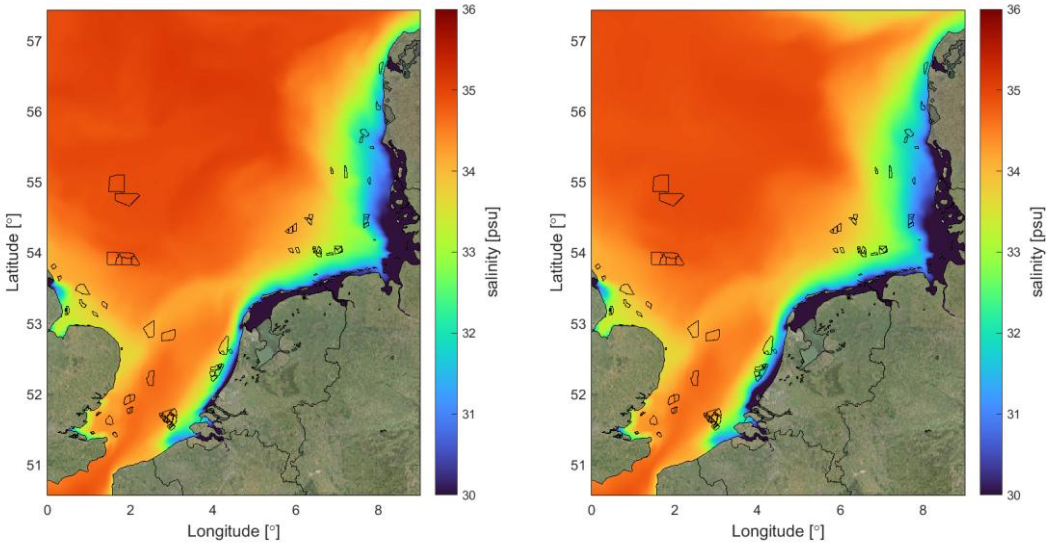

Figure 5.1 Annual mean bottom (left) and surface (right) salinity

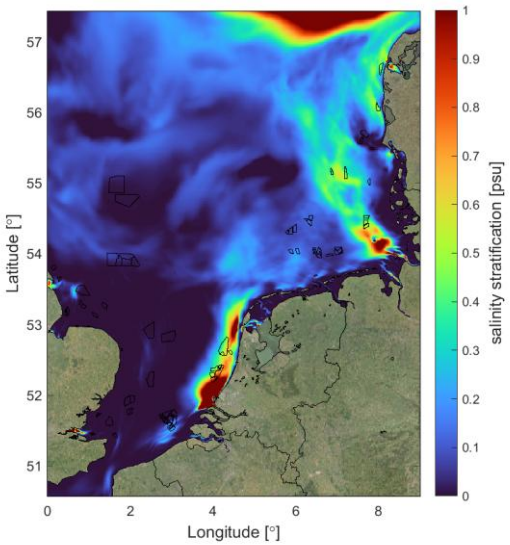

Figure 5.2 Annual mean salinity stratification

A.1.2 Temperature

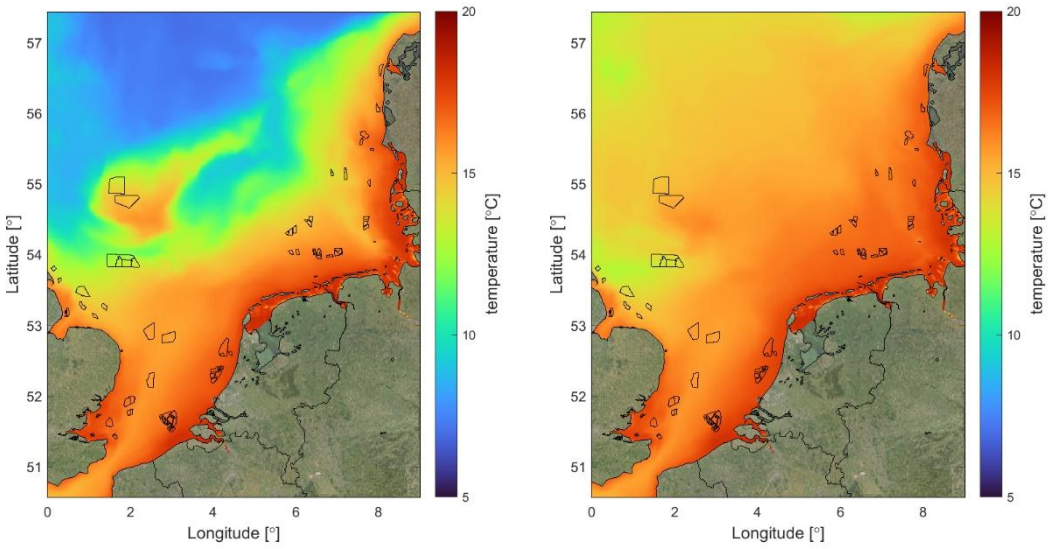

Figure 5.3 Annual mean bottom (left) and surface (right) temperature

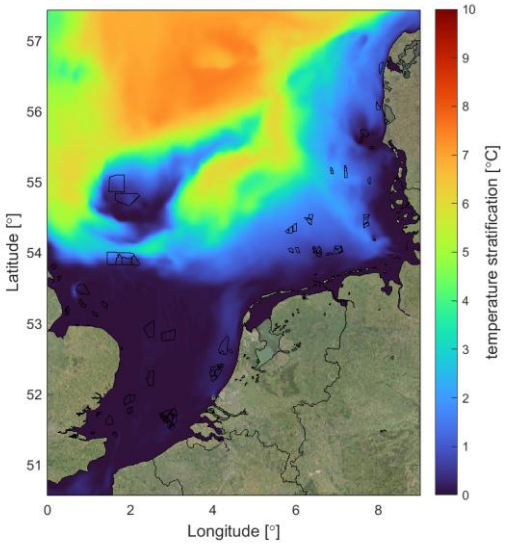

Figure 5.4 Annual mean temperature stratification

A.1.3 Residual currents

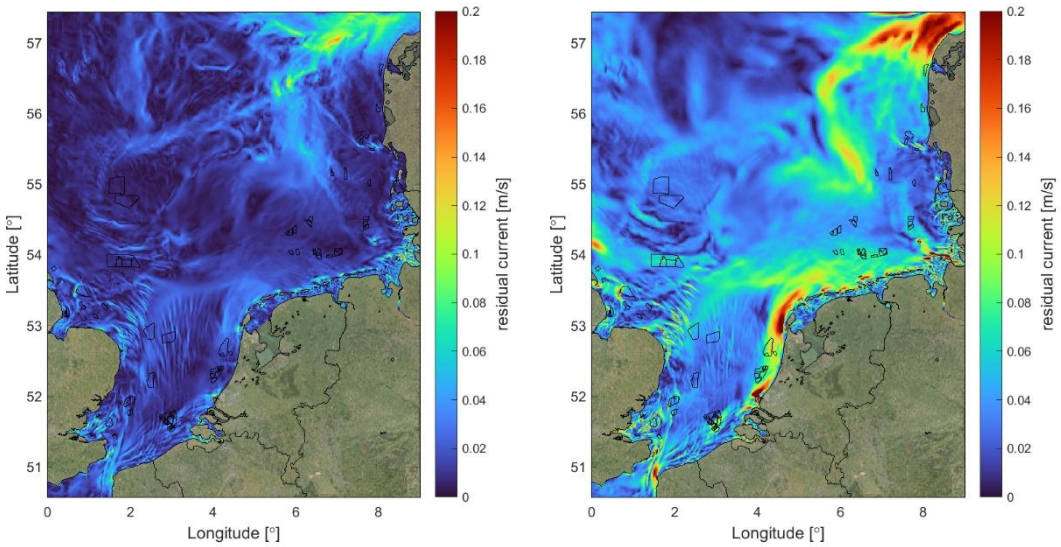

Figure 5.5 Annual mean residual current magnitude at bottom (left) and surface (right)

A.1.4 Bed shear stress

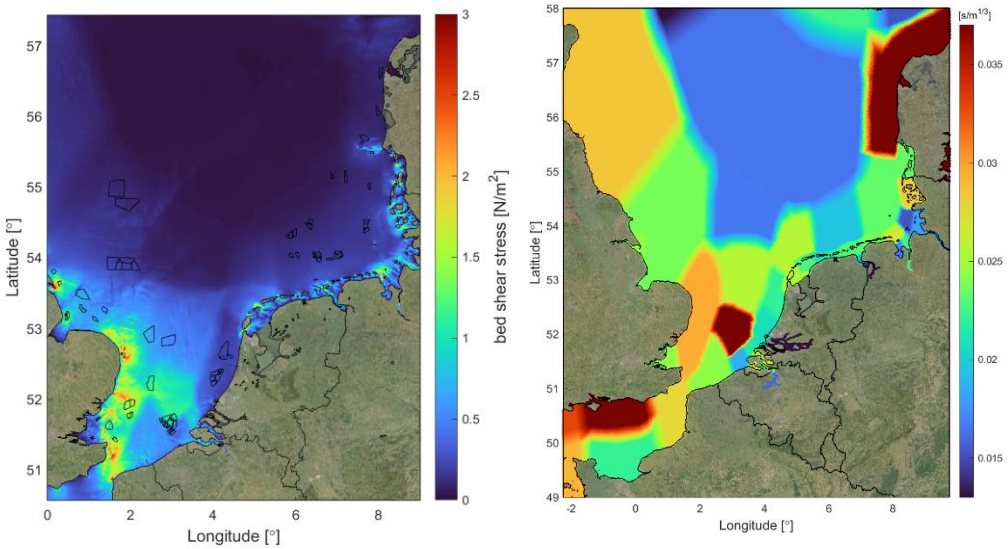

Figure 5.6 Annual mean bed shear stress (left) and calibrated roughness fields in the model (right)

A.2 Impact of the OWF2024 scenario (summer averages)

A.2.1 Salinity

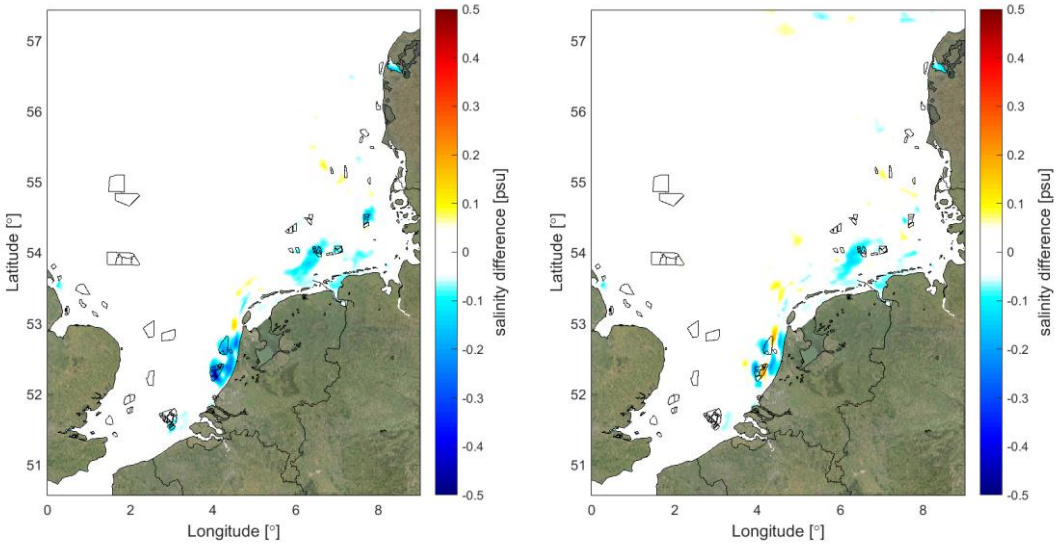

Figure 5.7 Change in mean bottom (left) and surface (right) salinity during summer due to the OWF2024 scenario; blue shows a decrease

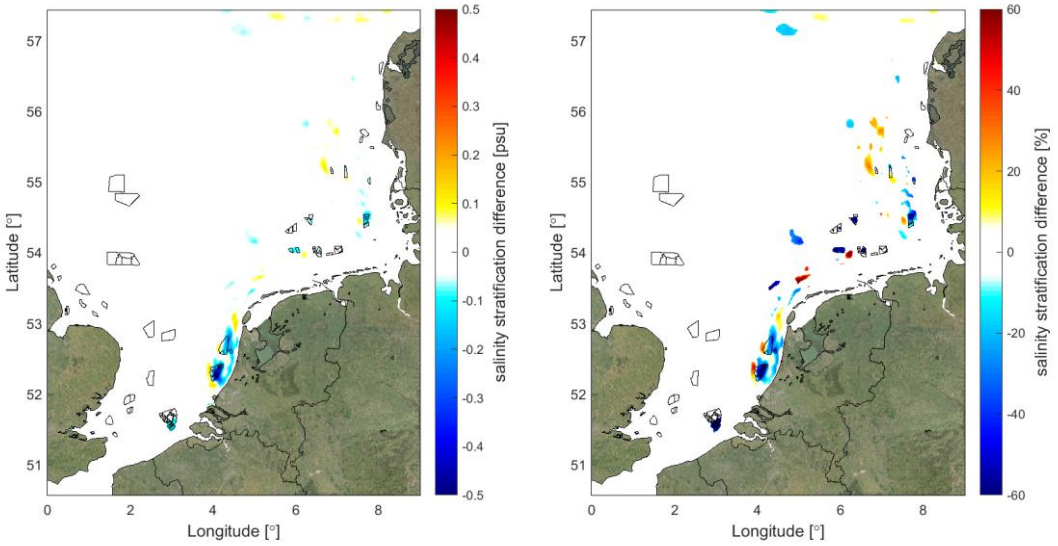

Figure 5.8 Absolute (left) and relative (right) change in mean salinity stratification during summer due to the OWF2024 scenario; blue shows a decrease

A.2.2 Temperature

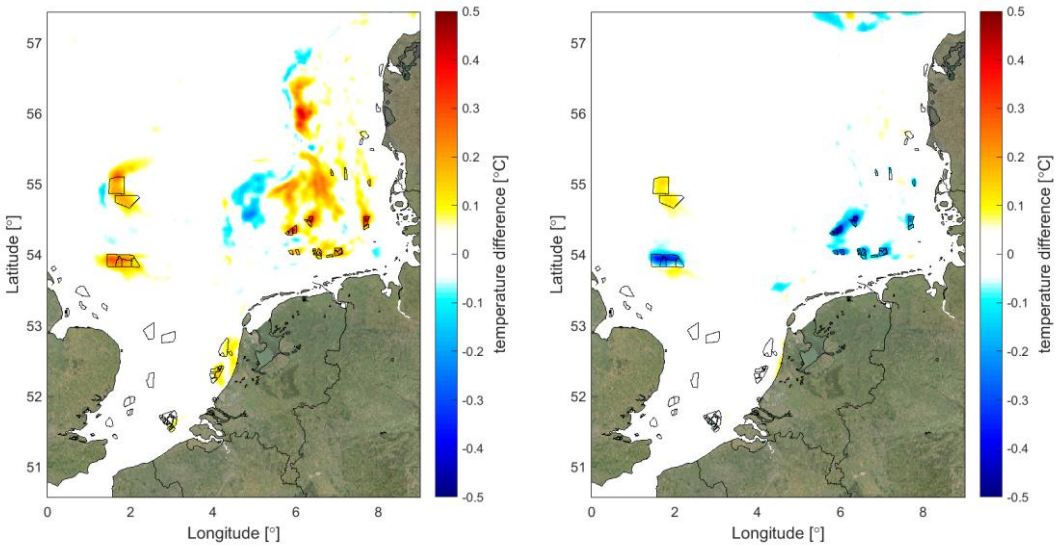

Figure 5.9 Change in mean bottom (left) and surface (right) temperature during summer due to the OWF2024 scenario; blue shows a decrease

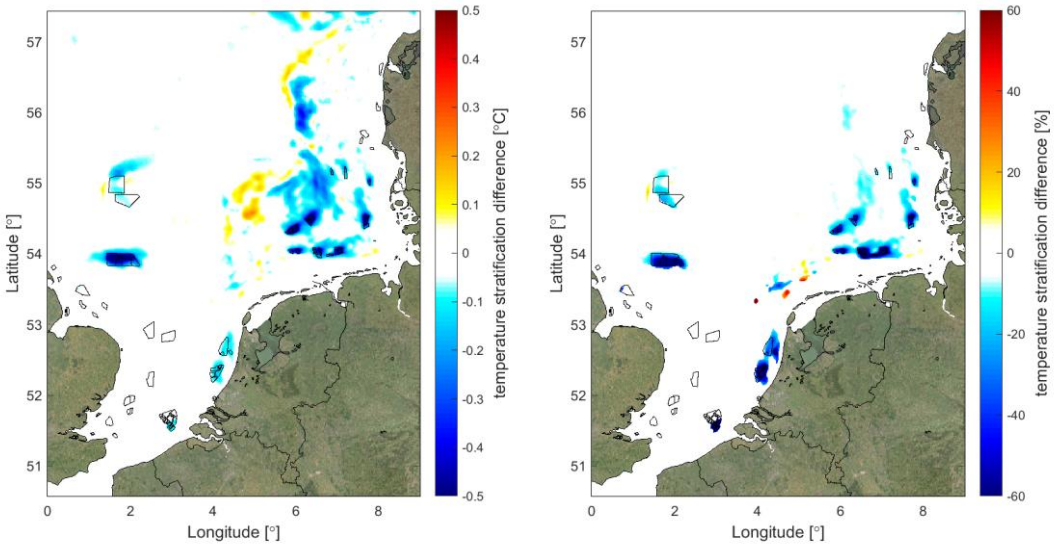

Figure 5.10 Absolute (left) and relative (right) change in mean temperature stratification during summer due to the OWF2024 scenario; blue shows a decrease

A.2.3 Residual currents

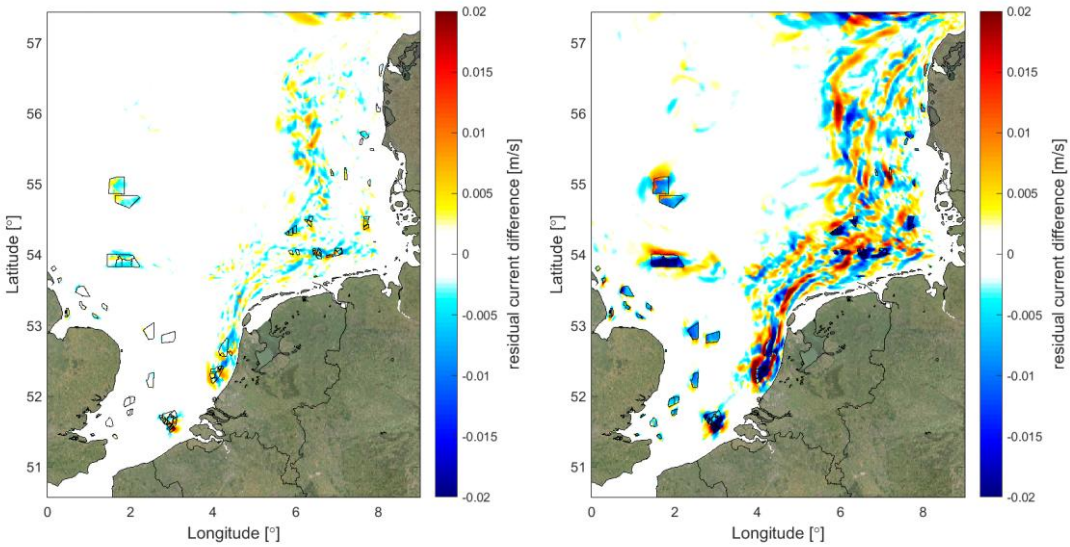

Figure 5.11 Change in mean bottom (left) and surface (right) velocity magnitude during summer due to the OWF2024 scenario; blue shows a decrease

A.2.4 Bed shear stress

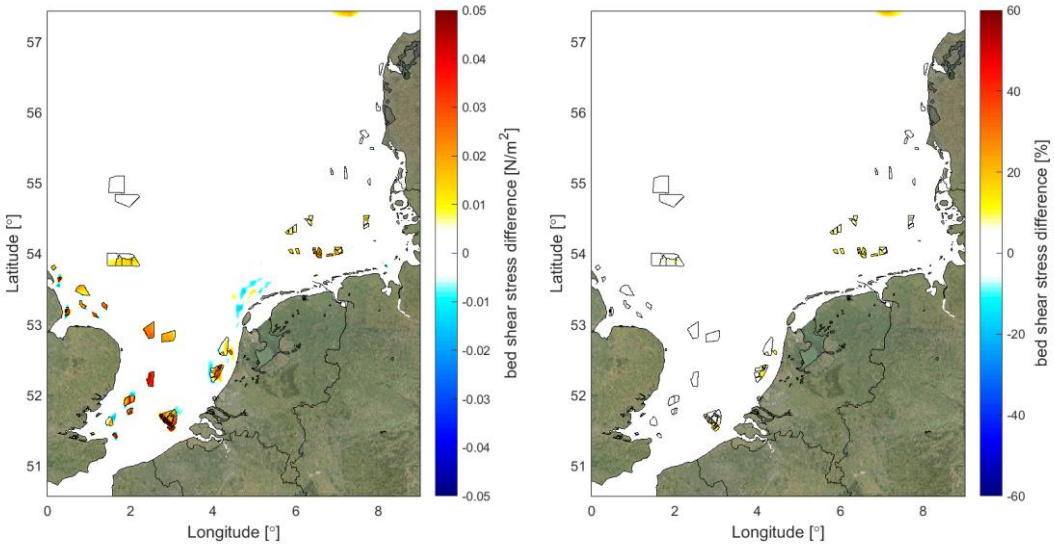

Figure 5.12 Absolute (left) and relative (right) change in mean bed shear stress during summer due to the OWF2024 scenario; blue shows a decrease

Deltares is an independent institute for applied research in the field of water and subsurface. Throughout the world, we work on smart solutions for people, environment and society.

Deltares

www.deltares.nl